Supplementary Information

Switchable supramolecular ensemble for anion binding with ditopic hydrogen-bonded macrocycles

Zejiang Liu‡, Kang Kang‡, Yidan Zhou, Rui Liu, Wen Feng, and Lihua Yuan*

Key Laboratory of Radiation Physics and Technology of the Ministry of Education, Institute of Nuclear Science and Technology, College of Chemistry, Sichuan University, Chengdu 610064, China.

‡These authors contributed equally to the work.

Contents

1. Materials and methods

The ^{1}H NMR and ^{13}C NMR spectra were recorded on Bruker AVANCE AV II-400 MHz (^{1}H: 400 MHz; ^{13}C: 100 MHz). $CDCl_3$, CD_3CN, and DMSO were purchased from Cambridge Isotope Laboratories, and were used for the titration experiments without further drying. Chemical shifts are reported in δ values in ppm using tetramethylsilane (TMS) and coupling constants (J) are denoted in Hz. Multiplicities are denoted as follows: s = singlet, d = doublet, t = triplet, dd = double doublet, and m = multiplet. High resolution mass (HRMS) data were collected by a WATERS Q-TOF Premier. All chemicals were obtained from commercial suppliers and were used as received unless otherwise noted. CH_2Cl_2 was dried over CaH_2. Column chromatography was carried out using silica gel (300 - 400 mesh). Solvents for chromatography were reagent grade.

2. Synthesis

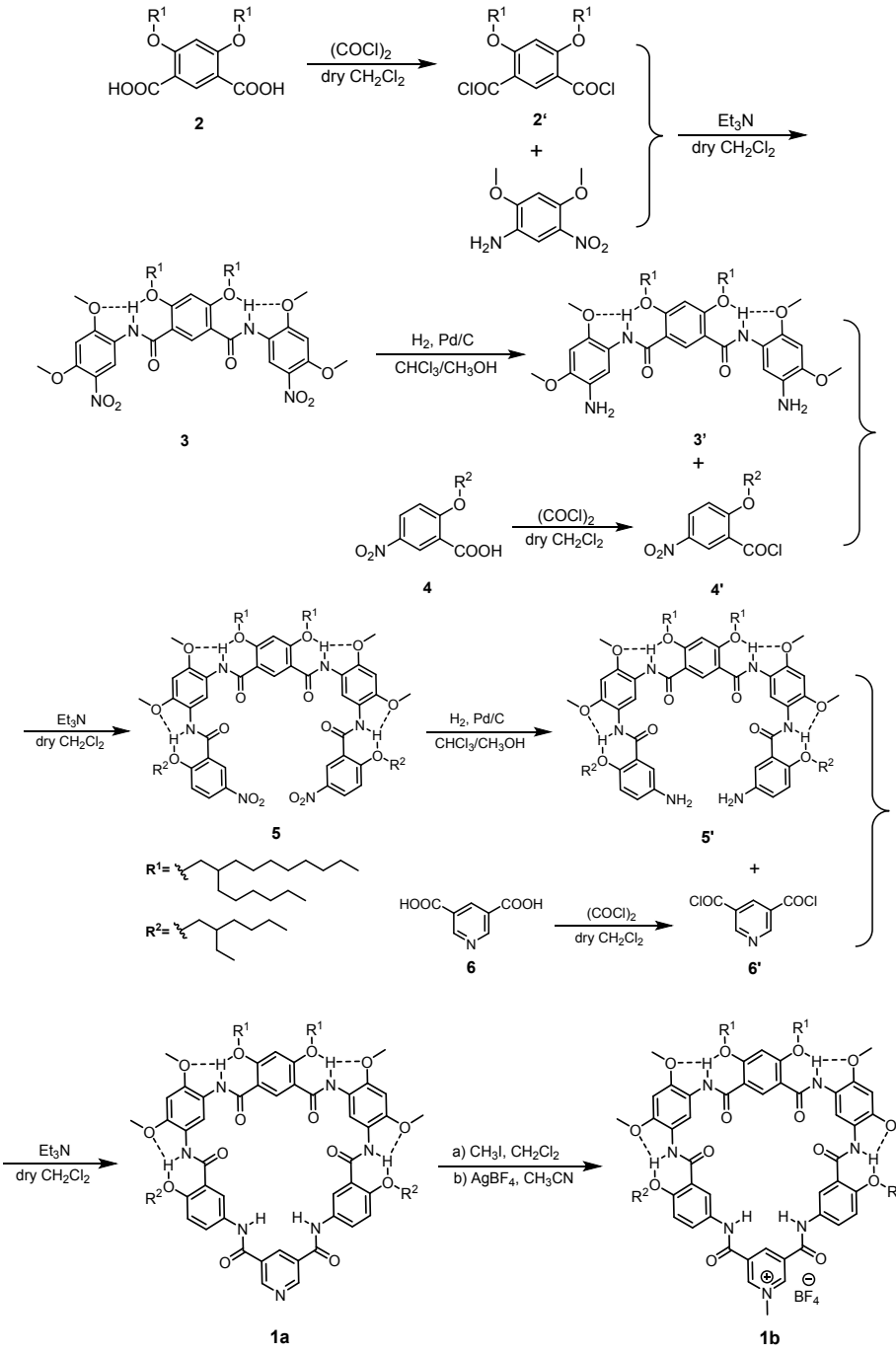

Scheme S1. Synthetic routes for macrocycles

Compounds **2-5** were synthesized according to analogous literature procedures. [28] **3** and **5** were converted into **3**' and **5**' by catalytic hydrogenation. Compounds **6**' were used directly in the subsequent reaction without further purification.

2.1 Synthesis of macrocycle 1a

Pentamer **5** (500 mg, 0.34 mmol) was hydrogenated in the presence of 25% Pd/C (125 mg) in $CHCl_3/CH_3OH$ (120 mL, 4:1, v/v) for 12 h at 45 ℃. The solution was filtered in darkness as fast as possible followed by immediate removal of the solvent. The reduced diamine was used for the immediate coupling reaction. DMF (5 uL) was added to a suspension of compound **6** (68 mg, 0.41 mmol) and oxalyl chloride (312 mg, 2.46 mmol) in CH_2Cl_2. The mixture was stirred for 40 min at room temperature. The solvent was evaporated and the resulting acid chloride was dried in vacuum at room temperature for 30 min to get compound **6'**. Compound **6'** was dissolved in CH_2Cl_2 (60 mL) and added dropwise to a mixture of the above **5a'** and Et_3N (101 mg, 1.00 mmol) in CH_2Cl_2 (20 mL) at 0 ℃. The solution was stirred under Ar for 2 h. The organic layer was washed with water (3 × 20 mL) and dried over anhydrous Na_2SO_4 and filtered. The crude product was purified by chromatography on silica gel (CH_2Cl_2/MeOH, 20: 1, v/v) to provide the product **1a** as a yellow solid (214 mg, 40.1%). Macrocycle **1a**: Yellow solid; ^{1}H NMR(400 MHz, $CDCl_3$, 298 K): δ= 10.14(s, 2H) 9.67 (s, 2H), 9.19 (s, 2H), 9.06 (s, 2H), 9.02 (s, 2H), 8.93 (s, 1H), 8.77 (s, 1H), 8.49 (dd, *J* = 9.0, 2.9 Hz, 2H), 8.22 (d, *J* = 2.9 Hz, 2H), 6.84 (d, *J* = 9.0 Hz, 2H), 6.41 (s, 2H), 4.15 (d, 4H), 4.00 – 3.89 (m, 10H), 3.78 (s, 6H), 2.05 (m, 2H), 1.94 (m, 2H), 1.63 – 1.07 (m, 88H).; ^{13}C NMR (100 MHz, $CDCl_3$, 298 K): δ 163.29, 162.20, 160.04, 153.26, 152.44, 146.87, 145.71, 132.45, 128.48, 122.07, 120.83, 119.20, 112.42, 77.37, 77.26, 77.06, 76.74, 72.39, 55.95, 55.23, 38.45, 37.75, 31.85, 31.84, 30.90, 30.05, 29.71, 29.68, 29.59, 29.57, 29.31, 28.58, 26.59, 23.06, 22.65, 22.63, 14.08, 14.06, 14.01, 10.22. MALDI-TOF-MS (m/z) calculated. for $C_{93}H_{133}N_7NaO_{14}^+$ $[M + H]^+$ 1572.994, found 1572.978

2.2 Synthesis of macrocycle 1b

Macrocycle **1a** (130 mg, 0.08mmol) was methylated in the presence of 5.0 equiv. CH_3I (58 mg, 0.40 mmol) in CH_2Cl_2 for 4 h at room temperature, after which a red solid was obtained by removal of the solvent. The counterion of the solid ion was exchanged with $AgBF_4$ in CH_2Cl_2/CH_3CN (50 mL, 4:1, v/v) and the solution phase was washed with water (3 × 20 mL). The crude product was purified by PTLC to provide the product **1b** as an orange solid (104 mg, 75%).Macrocycle **1b**: Orange solid; ^{1}H NMR(400 MHz, $CDCl_3$, 298 K): δ 10.95 (s, 2H), 10.01 (s, 1H), 9.93 (s, 2H), 9.70 (d, 4H), 9.61 (s, 2H), 8.95 (s, 1H), 8.68 (d, 2H), 8.09 (d, 2H), 7.39 (d, 2H), 6.93 (s, 1H), 6.88 (s, 2H), 4.54 (s, 4H), 4.32 (s, 5H), 4.20 (d, 5H), 3.95 (d, 15H), 2.51 (t, 56H) 2.01 (m, 6H), 1.33 (m, 88H), 0.94 (t, 9H), 0.82 (dt, 23H); ^{13}C NMR (101 MHz, $CDCl_3/CD_3OD$, 1:1, v/v, 298 K) δ 162.64, 160.89, 154.41, 149.18, 146.88, 146.26, 121.80, 119.71, 95.02, 78.27, 78.14, 77.95, 77.63, 73.55, 56.26, 50.11, 49.59, 49.38, 49.17, 48.95, 48.74, 48.53, 48.31, 39.02, 38.35, 32.29, 32.21, 31.51, 30.40, 30.10, 29.94, 29.71, 29.14, 27.05, 23.72, 23.51, 23.05, 14.29, 10.65.(There is no clear ^{13}C NMR spectrum even in the DMSO-d_6 due to the aggregation of macrocycle **1b**). MALDI-TOF-MS (m/z) calculated. for $C_{94}H_{136}N_7O_{14}^+$ $[M\text{-}BF_4^-]^+$ 1588.017, found 1588.307

3. ^{1}H NMR and ^{13}C NMR spectra of macrocycles 1a and 1b

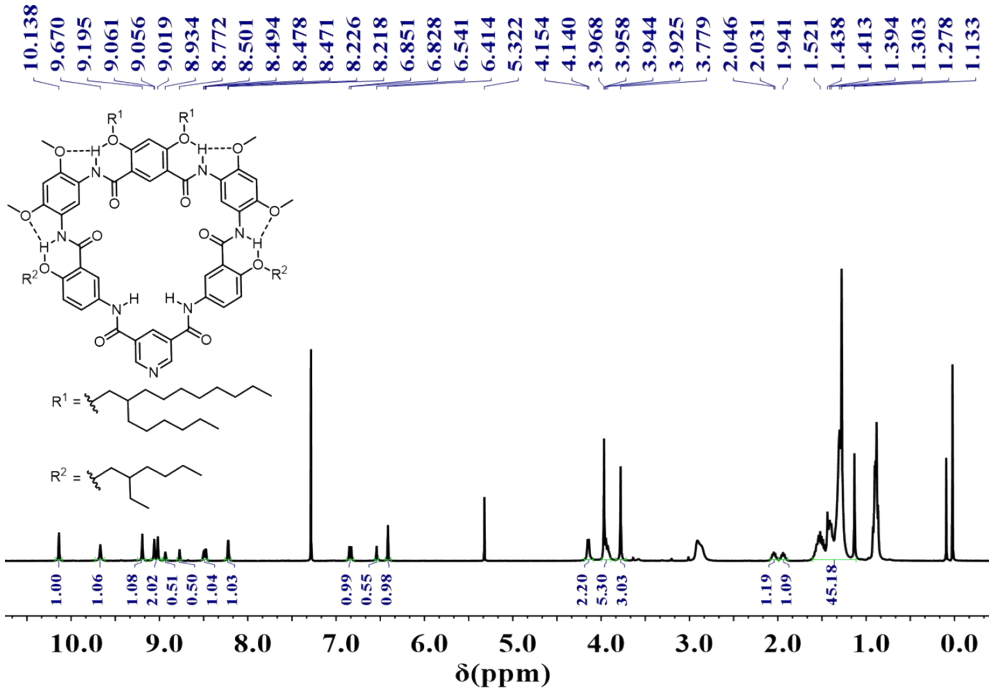

Figure S1. ^{1}H NMR spectrum of macrocycle **1a** (400 MHz, $CDCl_3$, 298 K)

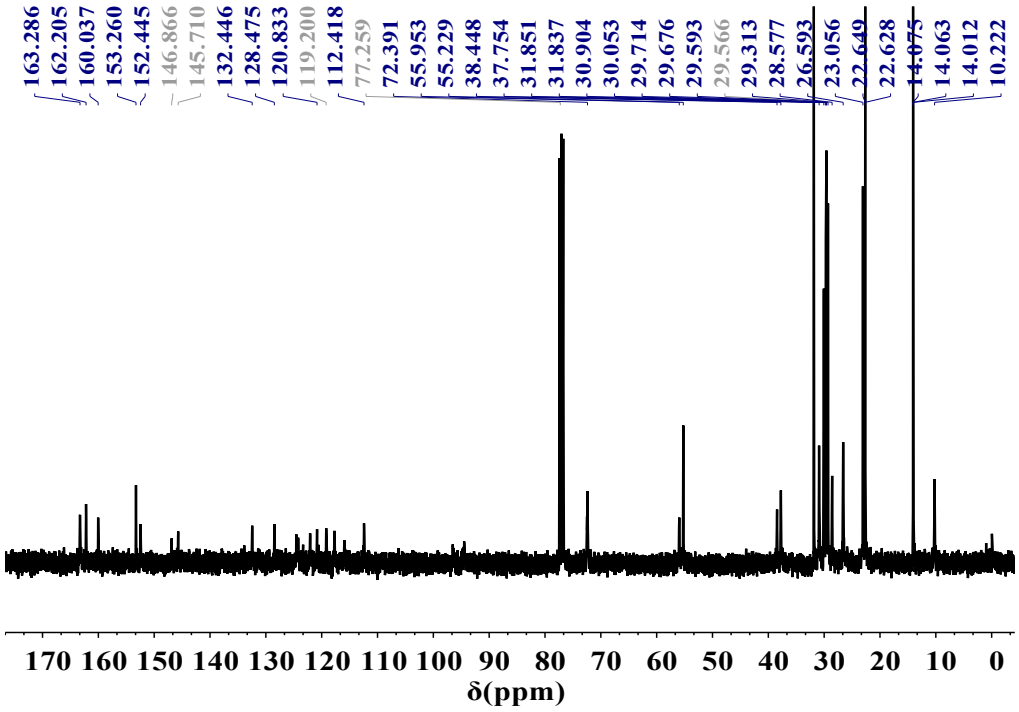

Figure S2. ^{13}C NMR spectrum of macrocycle **1a** (100 MHz, $CDCl_3$, 298 K)

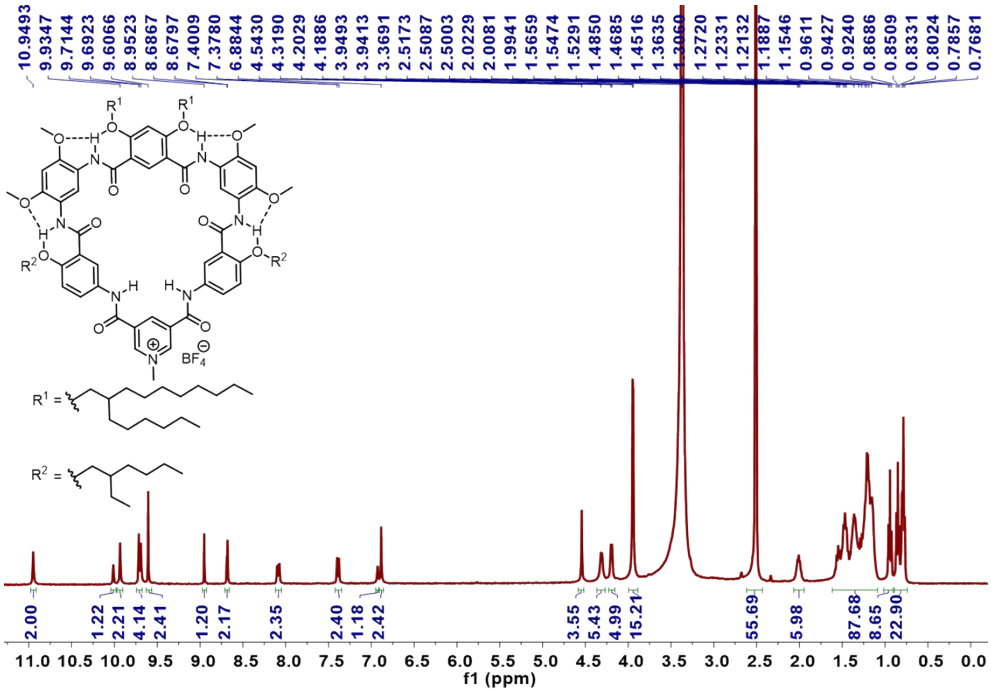

Figure S3. ^{1}H NMR spectrum of macrocycle **1b** (400 MHz, $CDCl_3$, 298 K)

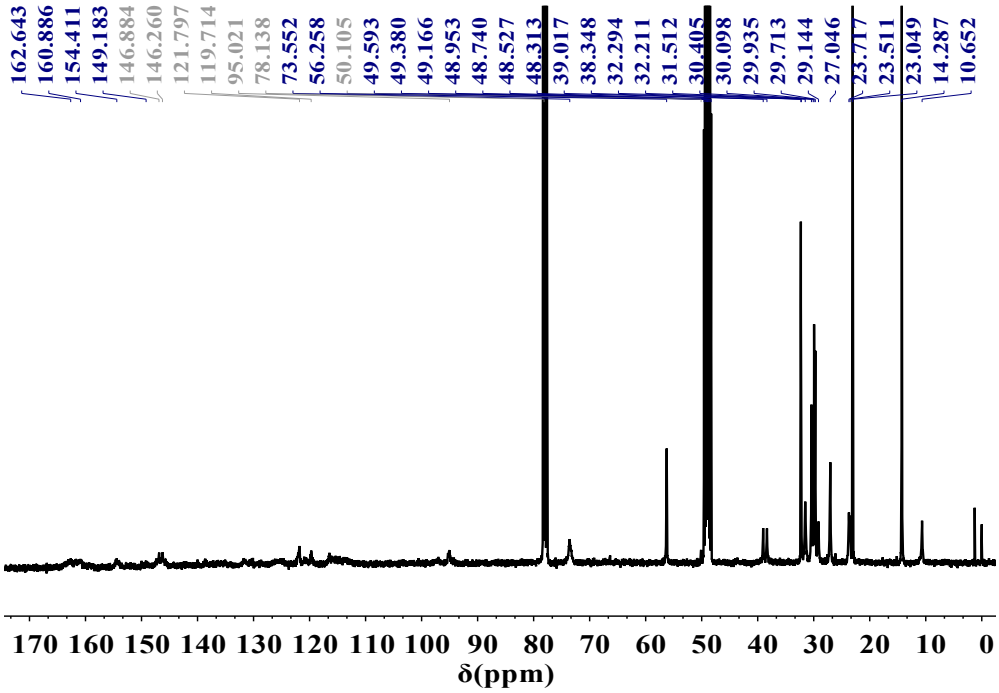

Figure S4. ^{13}C NMR spectrum of macrocycle **1b** (100 MHz, $CDCl_3$, 298 K)

4. Structure of pyridine-incorporated cyclo[6]aramide 1c

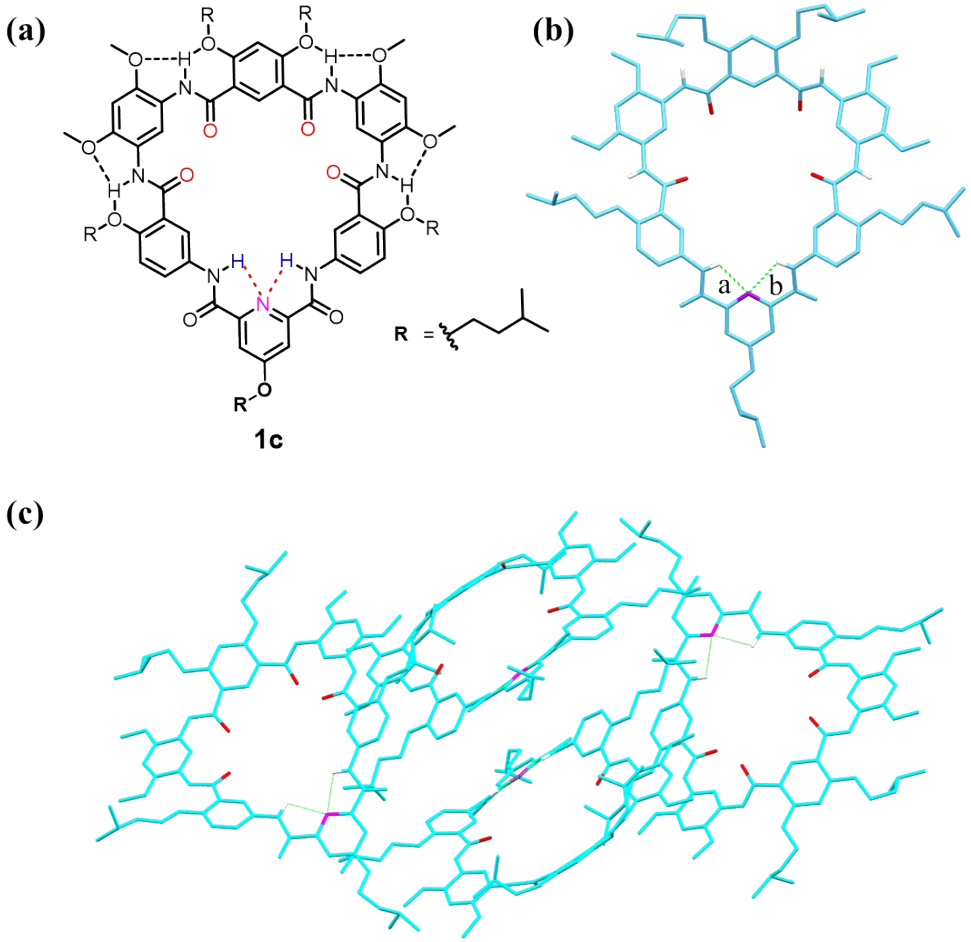

Figure S5. (a) Chemical structure of pyridine-incorporated cyclo[6]aramide **1c** (b) crystal structure of **1c** (c) packing mode of **1c** [37].

5. Proof of aggregation behavior in solution

5.1 Variable concentration ^{1}H NMR

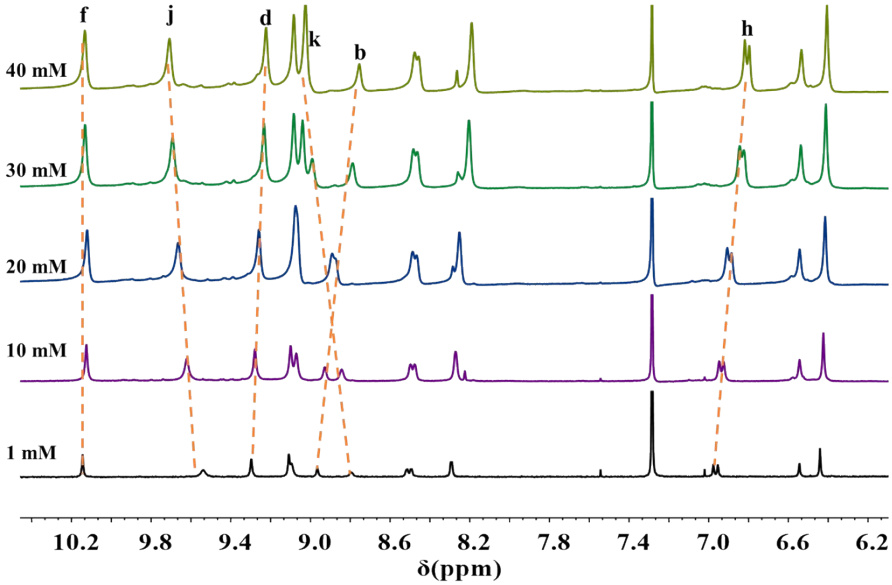

Figure S6. Variable concentration ^{1}H NMR spectra of macrocycle **1a** in $CDCl_3$ (400 MHz, 298 K).

5.2 UV spectra of macrocycles 1a and 1b

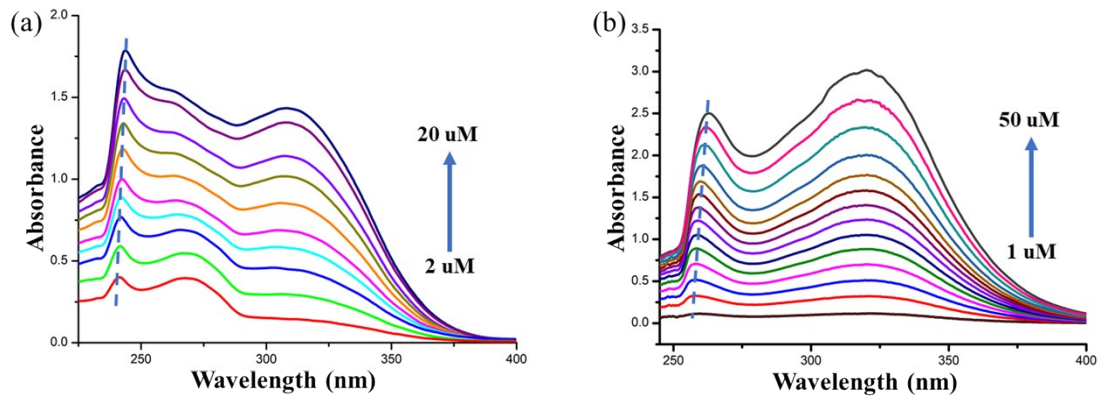

Figure S7. (a) Variable concentration UV spectra of macrocycle **1a** in $CHCl_3$. (b) Variable concentration UV spectra of macrocycle **1b** in $CHCl_3$/DMSO (1:1, v/v, 298 K).

5.3 DLS determination of macrocycle 1b

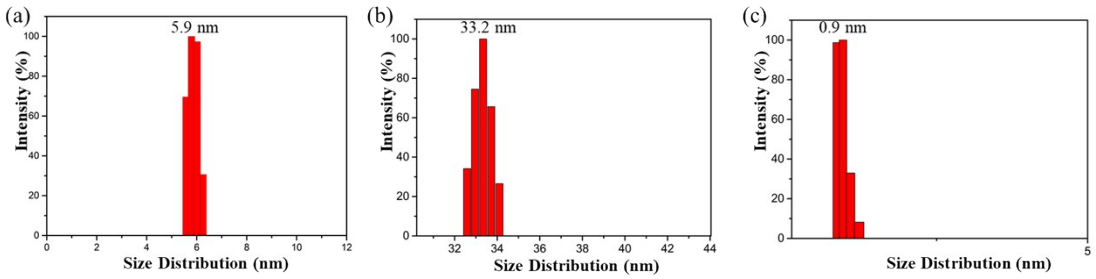

Figure S8. Aggregate size distribution of macrocycle **1b** in $CHCl_3$ at (a) 1 mM (b) 5 mM and (c)1 mM + 1.0 equiv $EMIMBF_4$

5. MALDI-TOF-MS spectra about macrocycles 1a and 1b

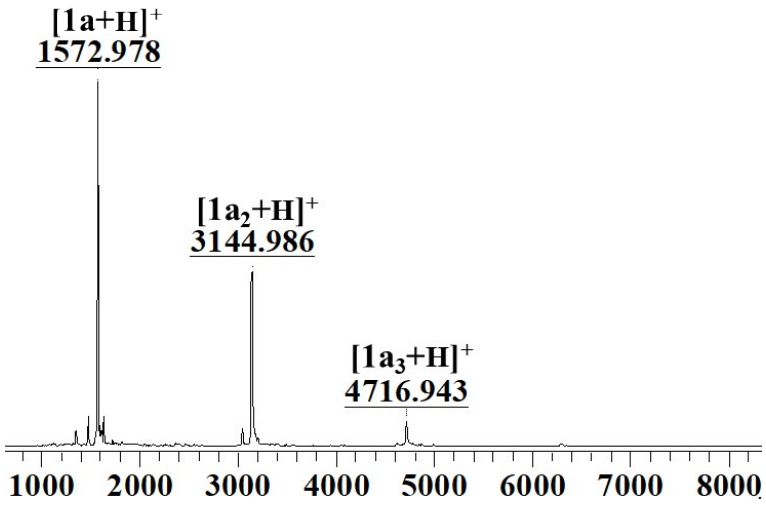

Figure S9. Partial MALDI-TOF mass spectrum of macrocycle **1a** (linear mode**)**

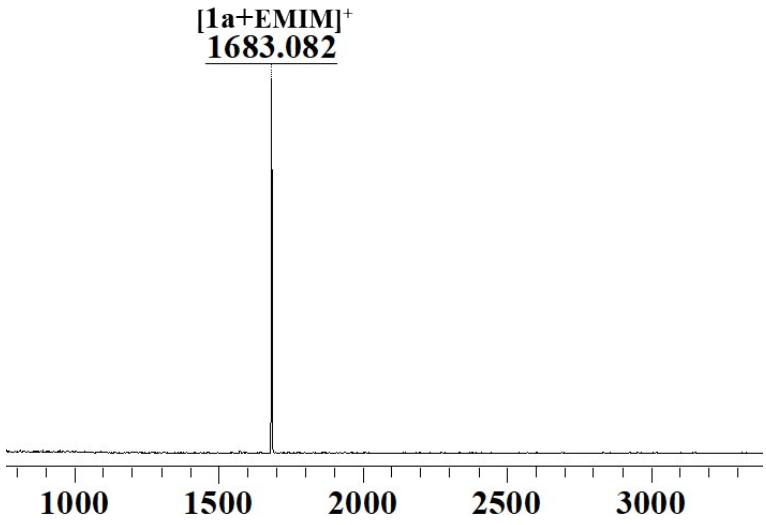

Figure S10. Partial MALDI-TOF mass spectrum of **1a** ⊃ $EMIMBF_4$ (reflection mode**)**

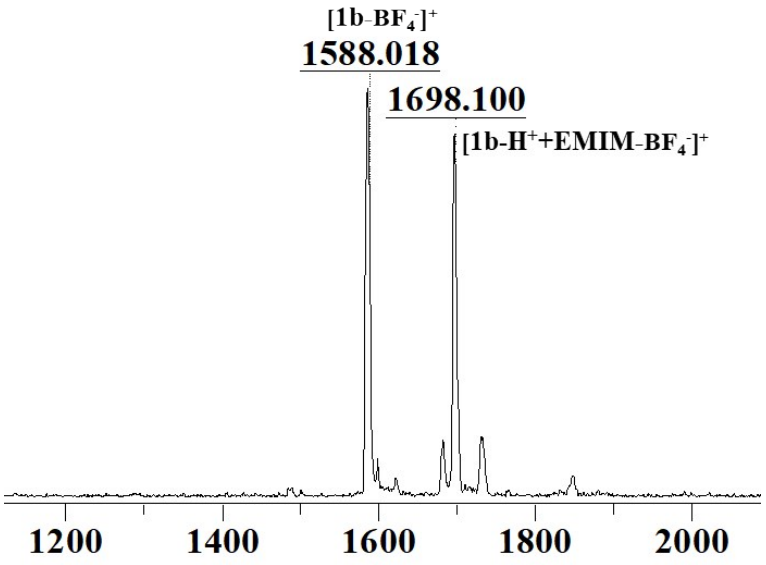

Figure S11. Partial MALDI-TOF mass spectrum of **1b** ⊃ $EMIMBF_4$ (linear mode**)**

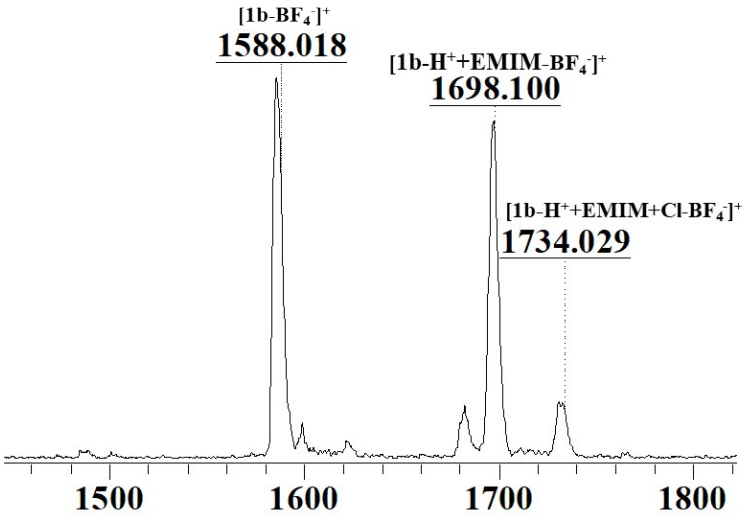

Figure S12. Partial MALDI-TOF mass spectrum of **1b** ⊃ EMIMCl (linear mode**)**

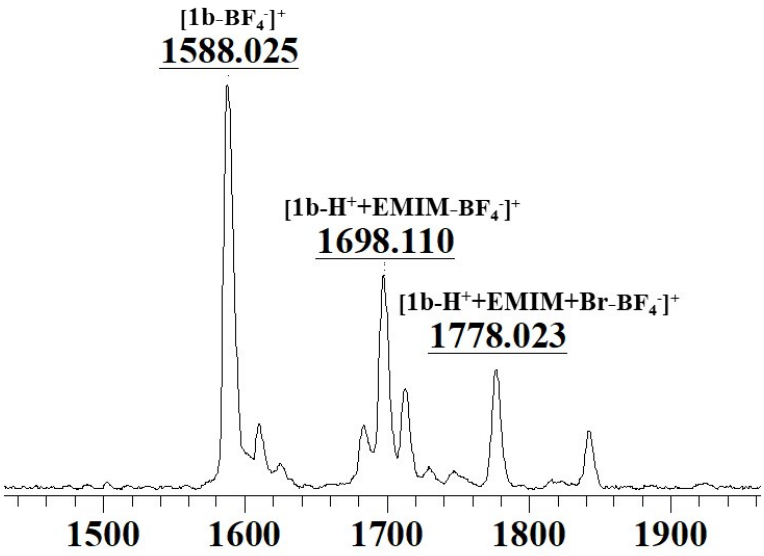

Figure S13. Partial MALDI-TOF mass spectrum of **1b** ⊃ EMIMBr (linear mode**)**

6. Single crystal structures of macrocycles 1a and 1b

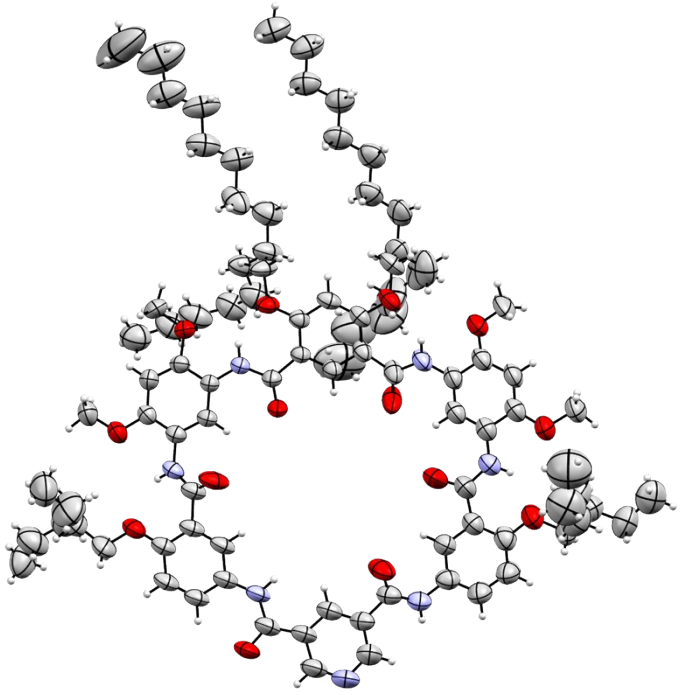

Figure S14. X-ray crystallographic analysis of macrocycle **1a** (displacement ellipsoids as drawn at the 50% probability level).

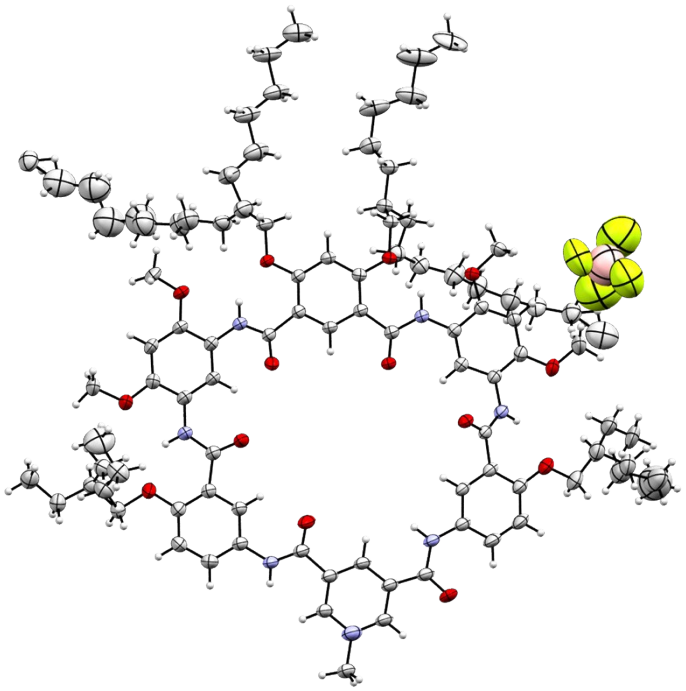

Figure S15. X-ray crystallographic analysis of macrocycle **1b** (displacement ellipsoids as drawn at the 50% probability level).

Table S1. Crystallographic data for macrocycles **1a** and **1b**

Crystal data	**1a**	**1b**
CCDC number	2083705	2083706
Empirical formula	$C_{97}H_{139}N_9O_{14}$	$C_{96}H_{139}BF_4N_8O_{14}$
Formula weight	1655.16	1715.95
Temperature/K	200.00(10)	100.01(10)
Crystal system	triclinic	triclinic
Space group	P-1	P-1
a/Å	13.4405(6)	13.29250(10)
b/Å	19.0973(5)	18.9665(2)
c/Å	20.3701(10)	21.1827(3)
α/°	70.575(3)	65.6240(10)
β/°	74.036(4)	77.3230(10)
γ/°	84.632(3)	84.4970(10)
Volume/Å^3	4740.7(4)	4745.69(10)
Z	2	2
ρ_{calc}g/cm^3	1.160	1.201
μ/mm^{-1}	0.617	0.691
F(000)	1792.0	1848.0
Crystal size/mm^3	? × ? × ?	? × ? × ?
Radiation	CuKα (λ = 1.54184)	CuKα(λ = 1.54184)
2Θ range for data collection/°	7.862 to 133.198	4.672 to 154.27
Index ranges	-15 ≤ h ≤ 15, -15 ≤ k ≤ 22, -24 ≤ l ≤ 24	-16 ≤ h ≤ 16, -23 ≤ k ≤ 23, -26 ≤ l ≤ 25
Reflections collected	28062	72579
Independent reflections	16569 [R_{int} = 0.0262, R_{sigma} = 0.0348]	19131 [R_{int} = 0.0341, R_{sigma} = 0.1193]
Data/restraints/parameters	16569/332/1173	19131/1529/1371
Goodness-of-fit on F^2	1.402	1.027
Final R indexes [I>=2σ (I)]	R_1 = 0.1205, wR_2 = 0.3601	R_1 = 0.0964, wR_2 = 0.2783

7. A probe into the combination of macrocycle 1 and guests

7.1 ^{1}H NMR determination of macrocycle 1b and different guests.

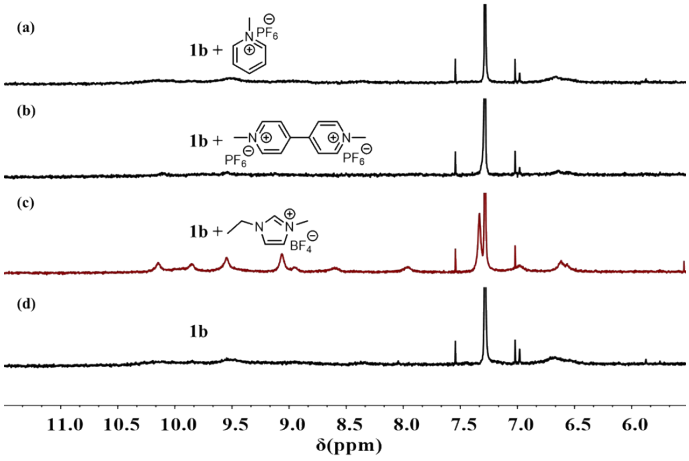

Figure S16. Stacked partial ^{1}H NMR spectra of (a) **1b** + 1.0 equiv **2c** (b) **1b** + 1.0 equiv **2b** (c) **1b** + 1.0 equiv **2a** (d) **1b** (1.0 mM, $CDCl_3$, 400 MHz, 298K)

7.2 2D-ROESY spectra of 1a and guest

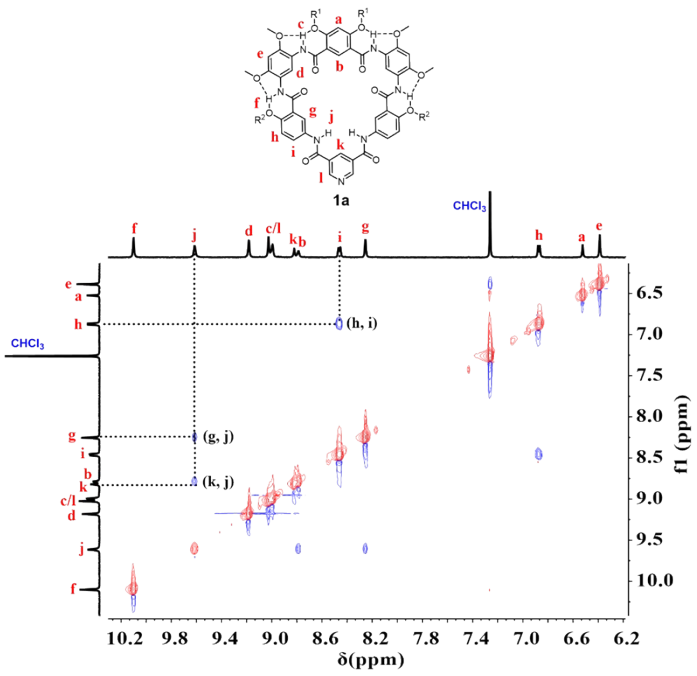

Figure S17. Expanded 2D ROESY spectrum of macrocycle **1a** (10 mM) ($CDCl_3$, 400 MHz, 298 K, mixing time = 0.4 s).

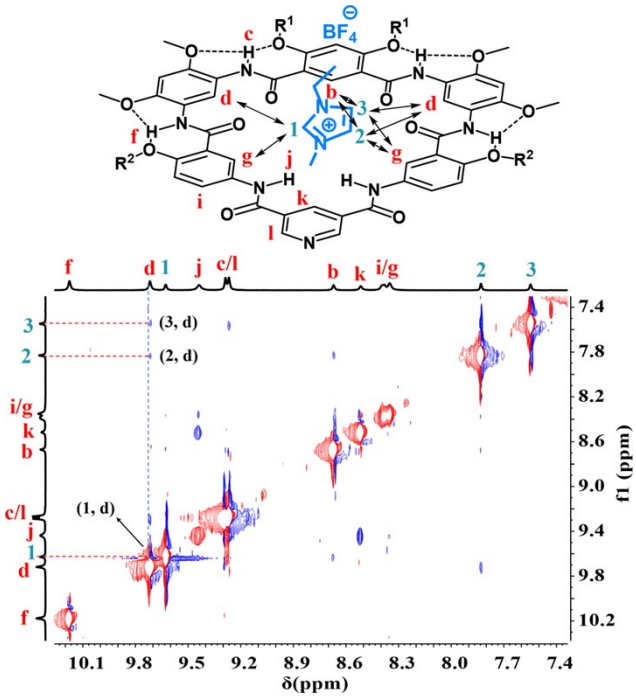

Figure S18. Expanded 2D ROESY spectrum of **1a** ⊃ EIMIMBF$_4$ (10 mM) (CDCl$_3$, 400 MHz, 298 K, mixing time = 0.4 s).

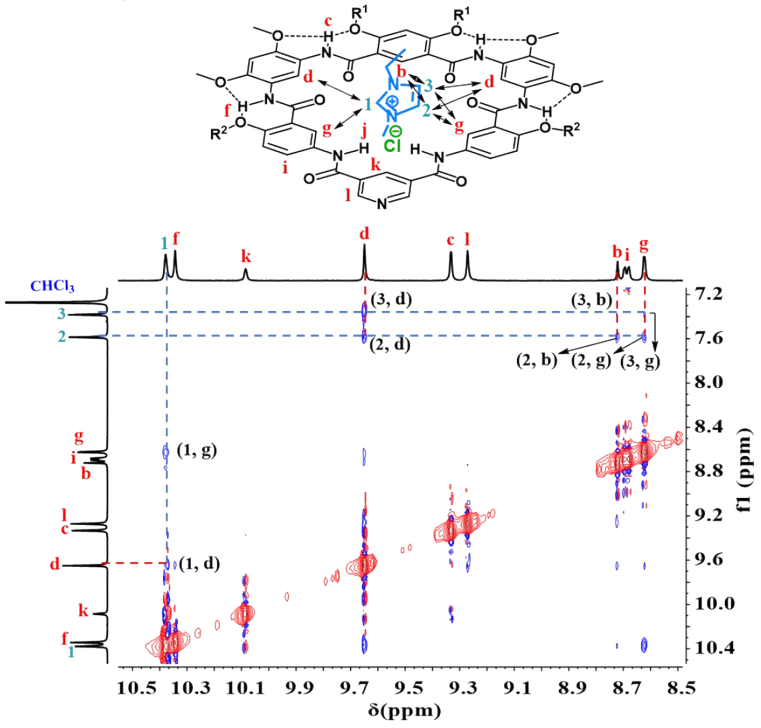

Figure S19. Expanded 2D ROESY spectrum of **1a** ⊃ EIMIMCl (10 mM) (CDCl$_3$, 400 MHz, 298 K, mixing time = 0.4 s).

7.3 2D-NOESY spectrum of macrocycle 1b

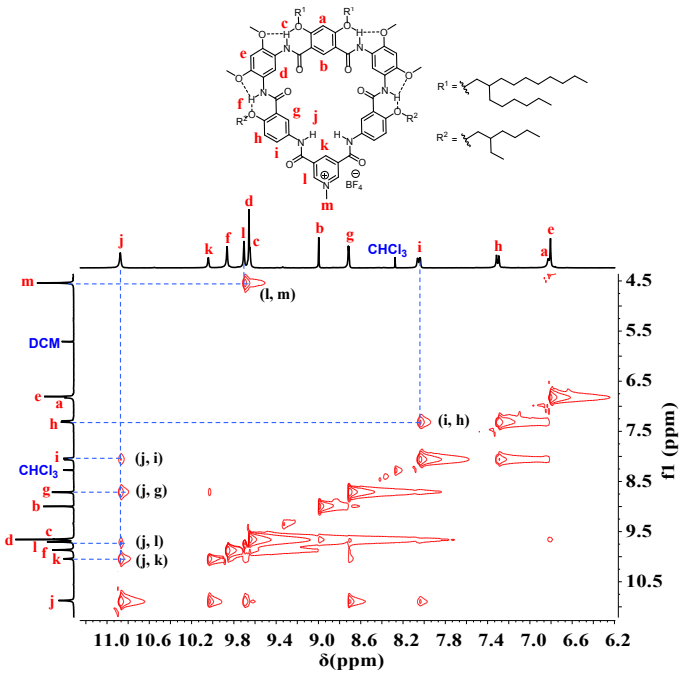

Figure S20. Expanded 2D NOESY spectrum of **1b** (10 mM) ($CDCl_3$: DMSO-d_6, 6:4, v/v, 400 MHz, 298 K, mixing time = 0.4 s).

7.3 Conformational optimization of macrocycle 1a with guest by ORCA

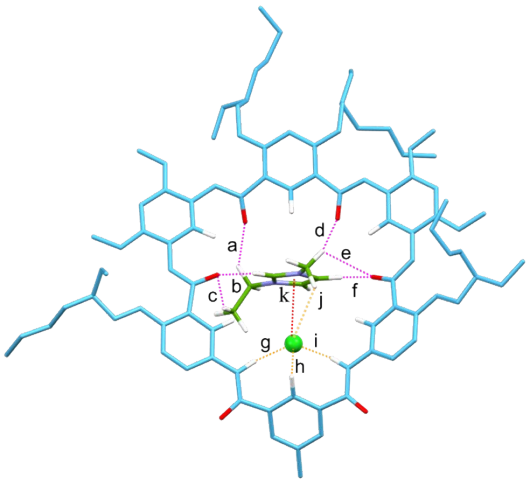

Figure S21. Top view of the optimized geometry of **1b** ⊃ $EMIMBF_4$ at the B97-3c level by ORCA. All side chains are simplified. a = 2.438 Å (134.11 °), b = 2.018 Å (170.45 °), c= 2.816 Å (148.78 °), d= 2.660 Å (127.01 °), e = 2.792 Å (106.55 °), f = 2.285 Å (142.12 °) g = 2.214 Å, h = 2.590 Å, i= 2.251 Å, j = 3.051 Å, k = 3.694 Å

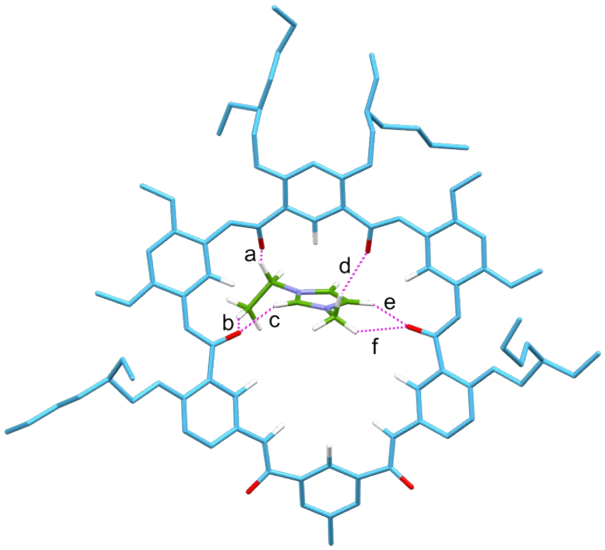

Figure S22. Top view of the optimized geometry of **1b** ⊃ $EMIMBF_4$ at the B97-3c level by ORCA. The tetrafluoroborate ions did not enter the cavity, so it has been omitted. All side chains are simplified. a = 2.421 Å (132.15 °), b = 2.746 Å (156.42 °), c= 2.104 Å (152.11 °), d= 2.501 Å (120.54 °), e = 2.344 Å (140.82 °), f = 2.407 Å (135.59 °)

8. Determination of catalytic yields

A solution of bromodiphenylmethane (5.0 mg, 20 μmol) in a mixture of solvents (2 mL, CH_2Cl_2/CH_3OH, 1: 1, v/v) was stirred in a reaction tube at room temperature. macrocycle **1b** (6.7 mg, 4 μmol), **2a** (3.9 mg, 20 μmol), and a mixture of macrocycle **1b** (6.7 mg, 4 μmol) and **2a** (3.9 mg, 20 μmol)was respectively added to the solution above, followed by stirring at different temperatures for 8h. Yellow precipitation was removed after adding excess CH_3CN. The filtrate after removal of solvents was subjected to ^1H NMR determination for yields of diphenyl(methoxy)methane in the presence of 1,1,2,2-tetrachloroethane (1.7 mg 10 μmol) as the internal standard.

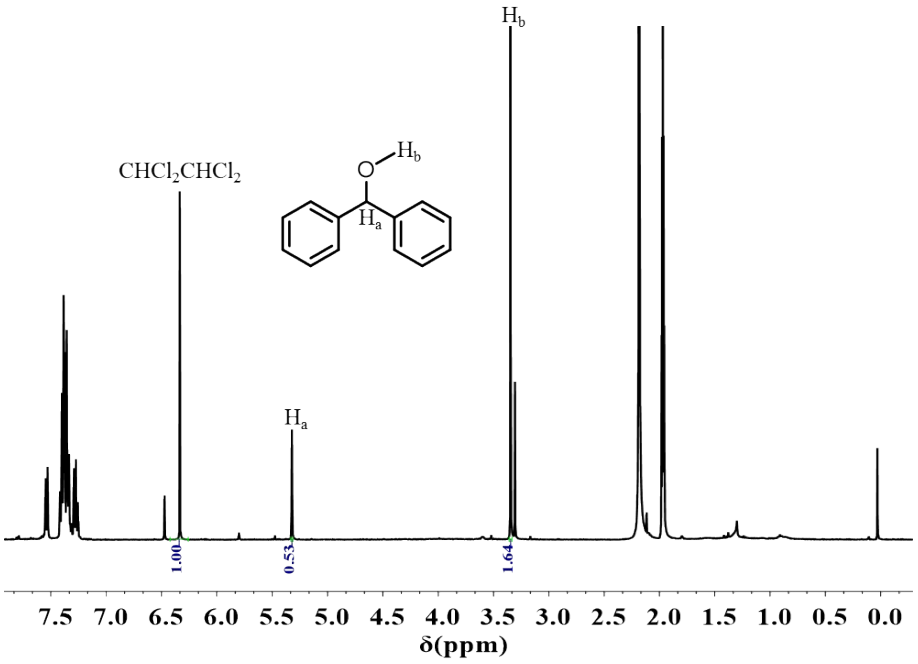

Figure S23. ^{1}H NMR spectrum of reaction mixture of bromodiphenylmethane after stirring for 8 h in 25℃ (400 MHz, CD_3CN, 298 K).

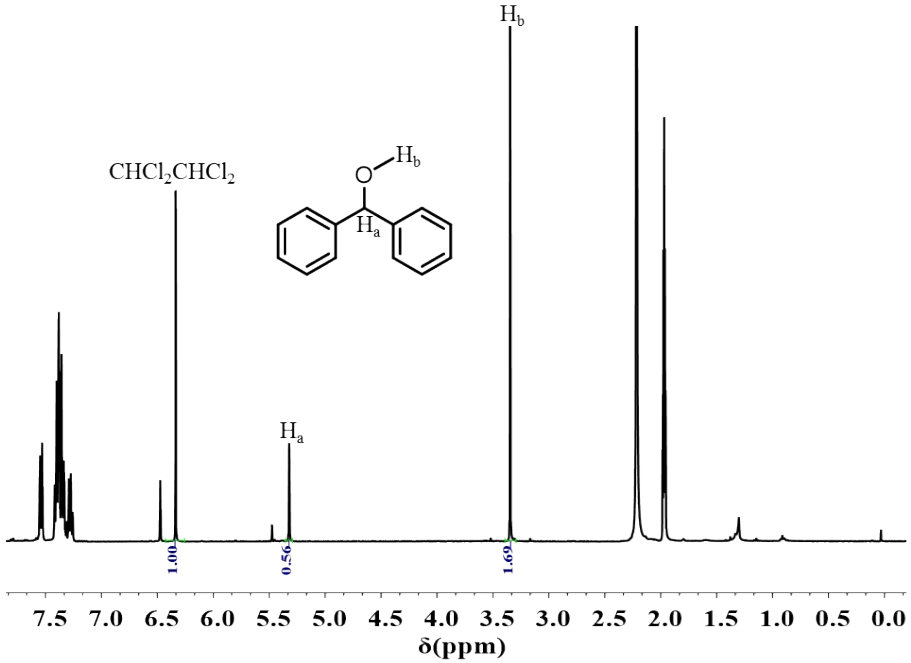

Figure S24. ^{1}H NMR spectrum of reaction mixture of bromodiphenylmethane and 20 mol% of **1b** after stirring for 8 h in 25℃ (400 MHz, CD_3CN, 298 K).

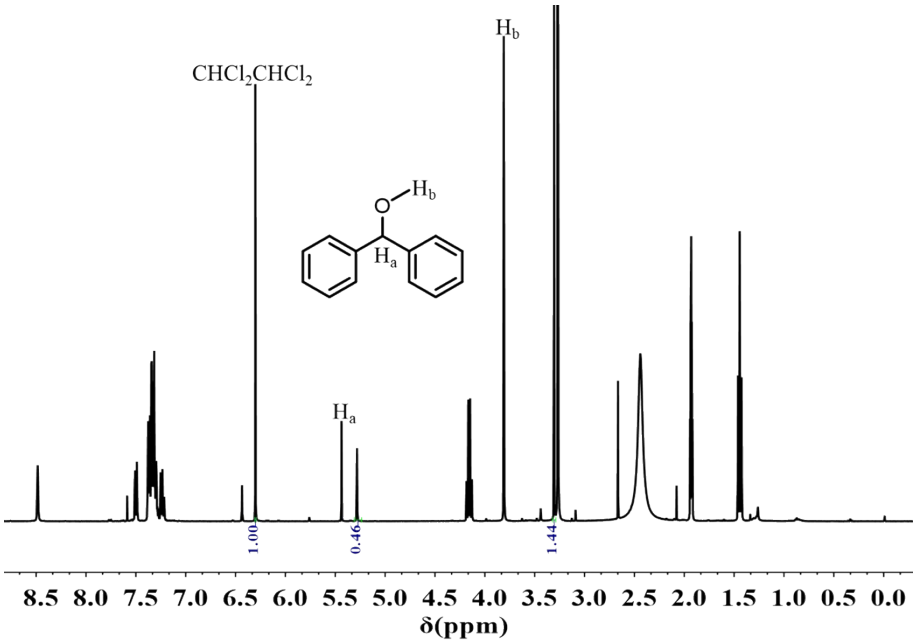

Figure S25. ^{1}H NMR spectrum of reaction mixture of bromodiphenylmethane and 100 mol% of **2a** after stirring for 8 h in 25℃ (400 MHz, 298 K).

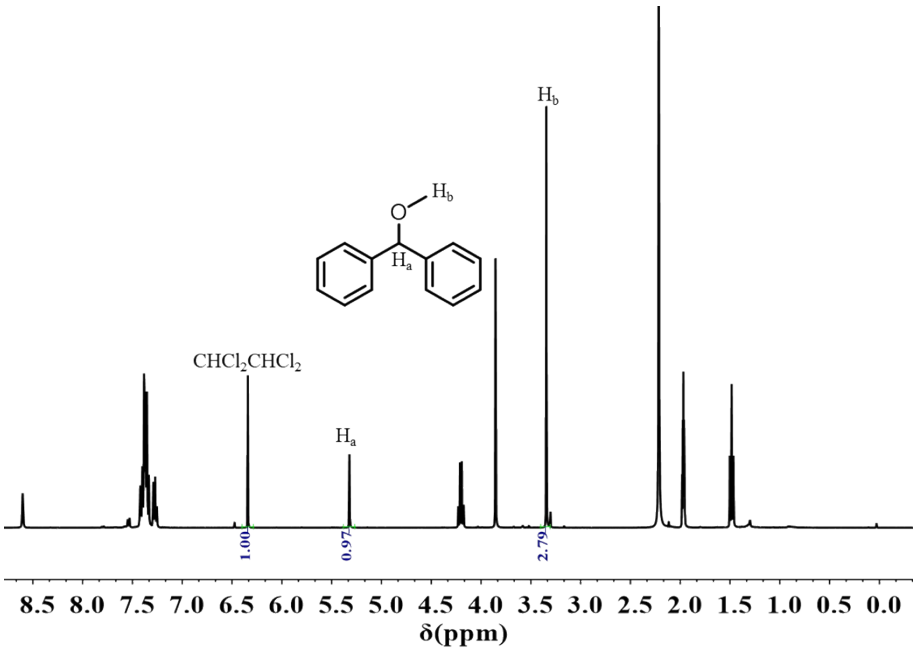

Figure S26. ^{1}H NMR spectrum of reaction mixture of bromodiphenylmethane, 20 mol% of **1b** and 100 mol% of **2a** after stirring for 8 h in 25℃ (400 MHz, 298 K).

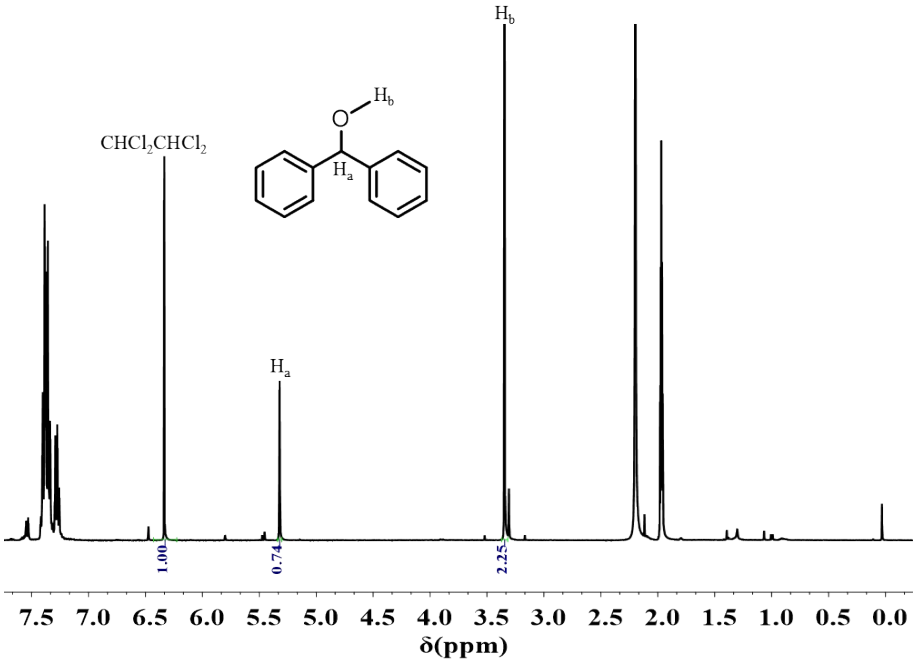

Figure S27. ^{1}H NMR spectrum of reaction mixture of bromodiphenylmethane after stirring for 8 h in 50 ℃ (400 MHz, CD_3CN, 298 K).

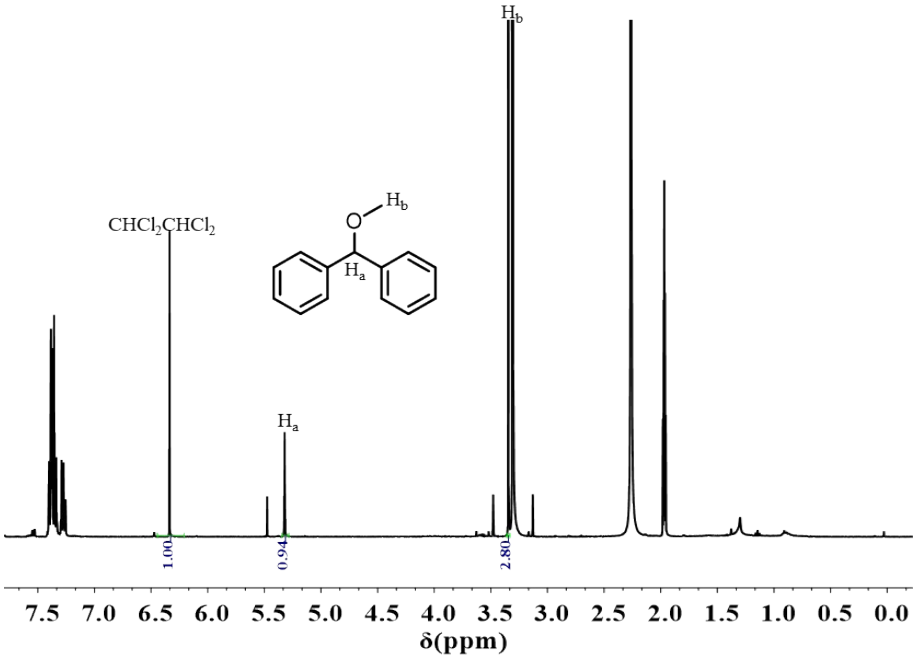

Figure S28. ^{1}H NMR spectrum of reaction mixture of bromodiphenylmethane and **1b** after stirring for 8 h in 50 ℃ (400 MHz, CD_3CN, 298 K).

9. Experimental comparison of non-aggregating macrocycle 1d

9.1 Synthesis of macrocycle 1d

Macrocycle **1d** were synthesized according to analogous literature procedures. [28]: Yellow solid: ^{1}H NMR (400 MHz, Chloroform-d) δ 10.10 (s, 2H), 9.47 (s, 2H), 9.30 (s, 2H), 9.23 (s, 2H), 8.81 (s, 2H), 8.42 (d, 2H), 8.35 (d, 2H), 7.91 (s, 2H), 7.67 (s, 2H), 7.10 (d, 2H), 6.49 (s, 1H), 6.48 (s, 2H), 4.08 (dd, 8H), 3.88 (m, 12H), 2.00 (m, 4H), 1.76 (m, 1H), 1.08 (m, 102H).

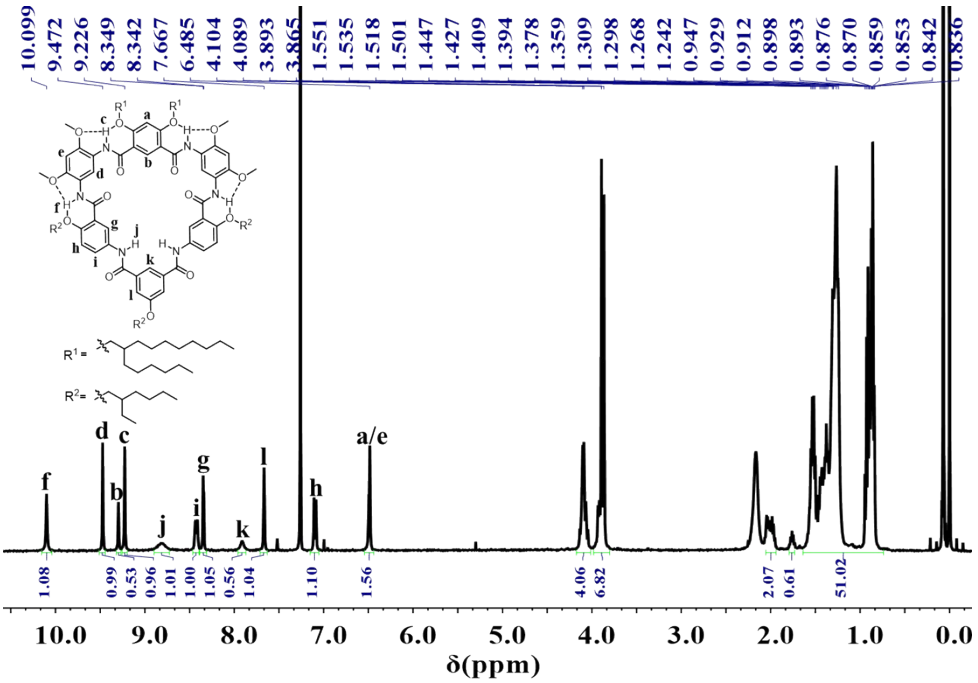

Figure S29. ^{1}H NMR spectrum of **1d** (400 MHz, $CDCl_3$, 298 K).

9.2 UV job plot experiment

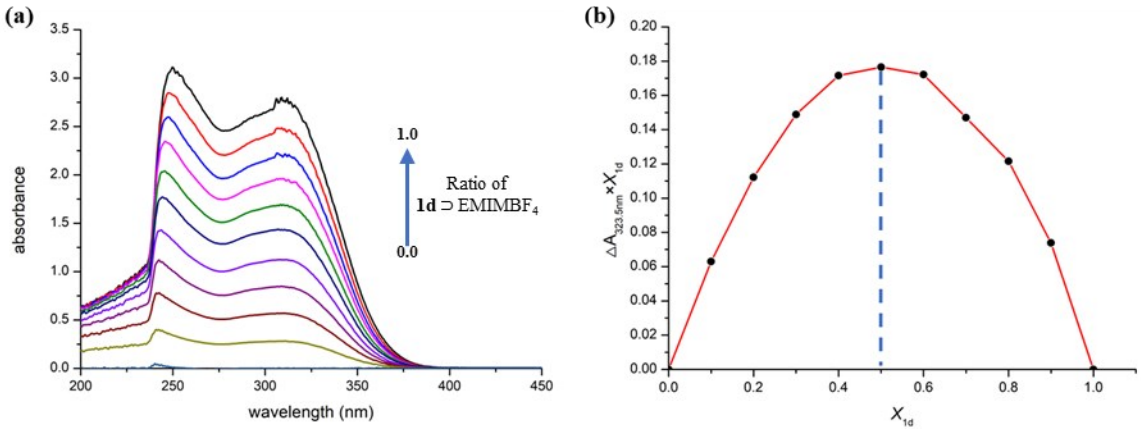

Figure S30. (a) Stacked plots of UV spectra of **1d** ⊃ $EMIMBF_4$ with TBABr at different concentration in $CHCl_3$, (b) Job plots between **1d** ⊃ $EMIMBF_4$ and TBABr were obtained by plotting the changes of absorbance on **1d** at 323.5 nm indicating a 1:1 stoichiometry.

9.3 ^{1}H NMR titration of macrocycle 1d

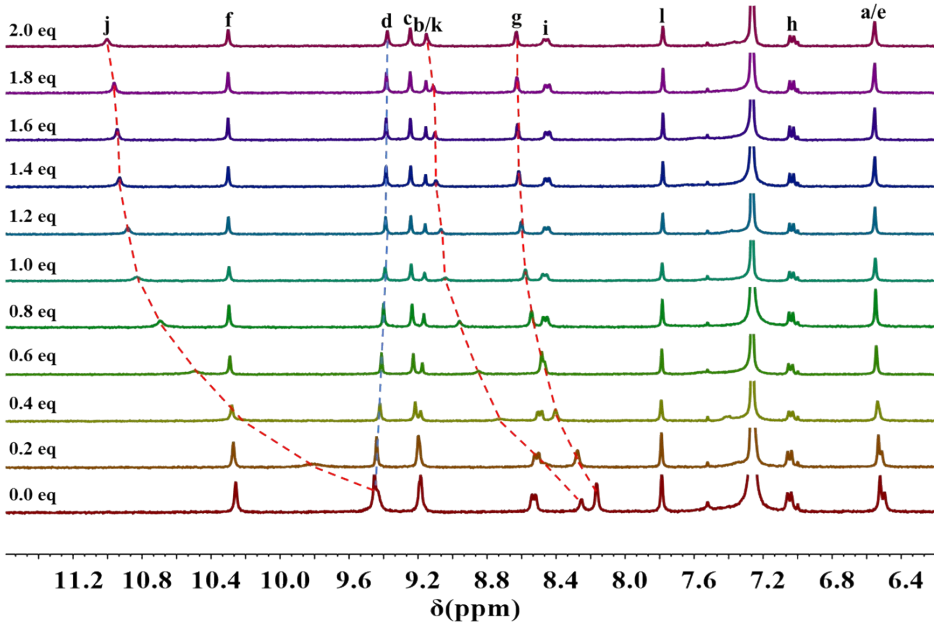

Figure S31. Stacked partial ^{1}H NMR spectra of (a) **1d** (1.0 mM) and (b) with TBABr at different concentration in $CDCl_3$ (400 MHz, 298 K).

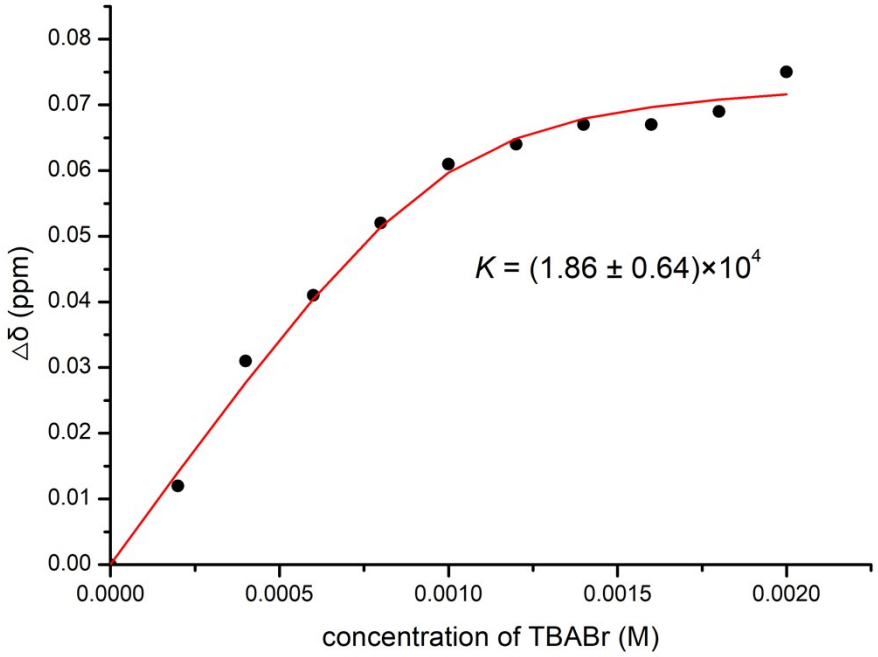

Figure S32. Determination of the binding conctant of **1d** • TBABr in $CDCl_3$ at 298K. Fitting result based on proton d of macrocycle **1d**

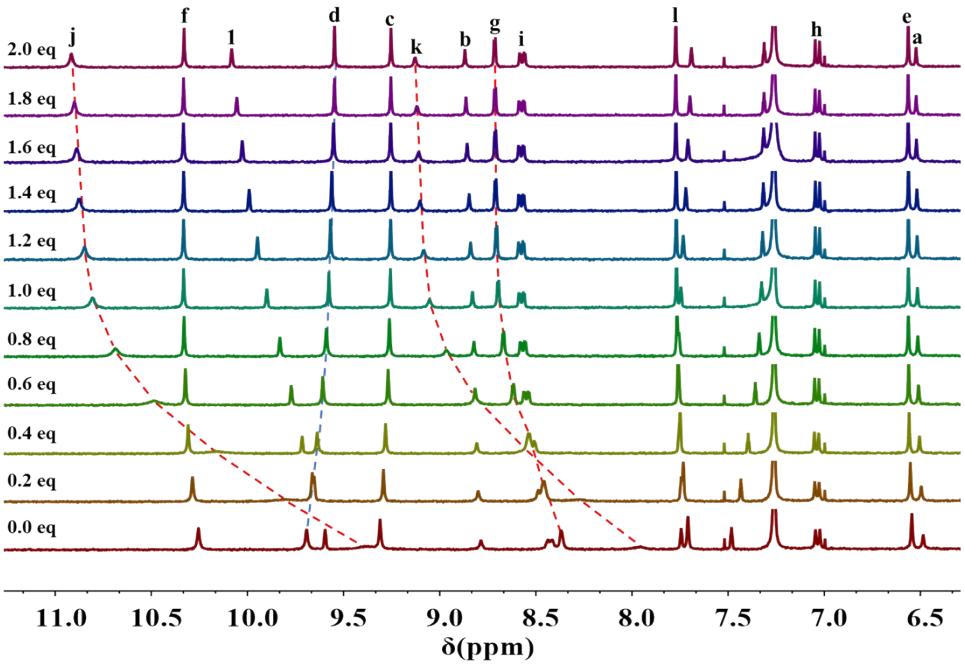

Figure S33. Stacked partial ^{1}H NMR spectra of (a) **1d** ⊃ $EMIMBF_4$ (1.0 mM) and (b) with TBABr at different concentration in $CDCl_3$ (400 MHz, 298 K).

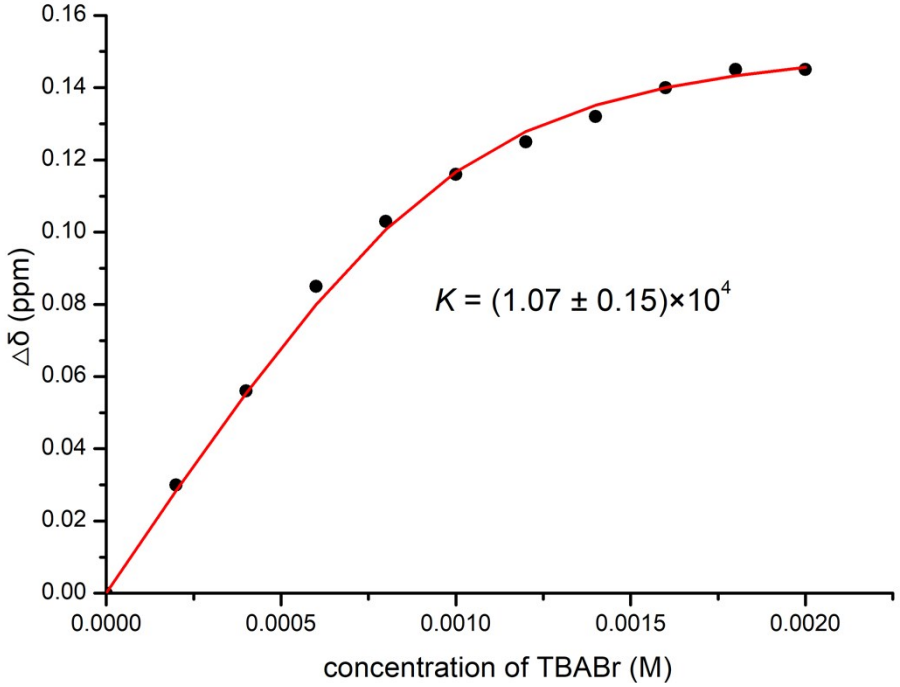

Figure S34. Determination of the binding conctant of **1d** ⊃ $EMIMBF_4$ • TBABr in $CDCl_3$ at 298K. Fitting result based on proton d of macrocycle **1d**

10. ^{1}H NMR titration of macrocycles 1a and 1b

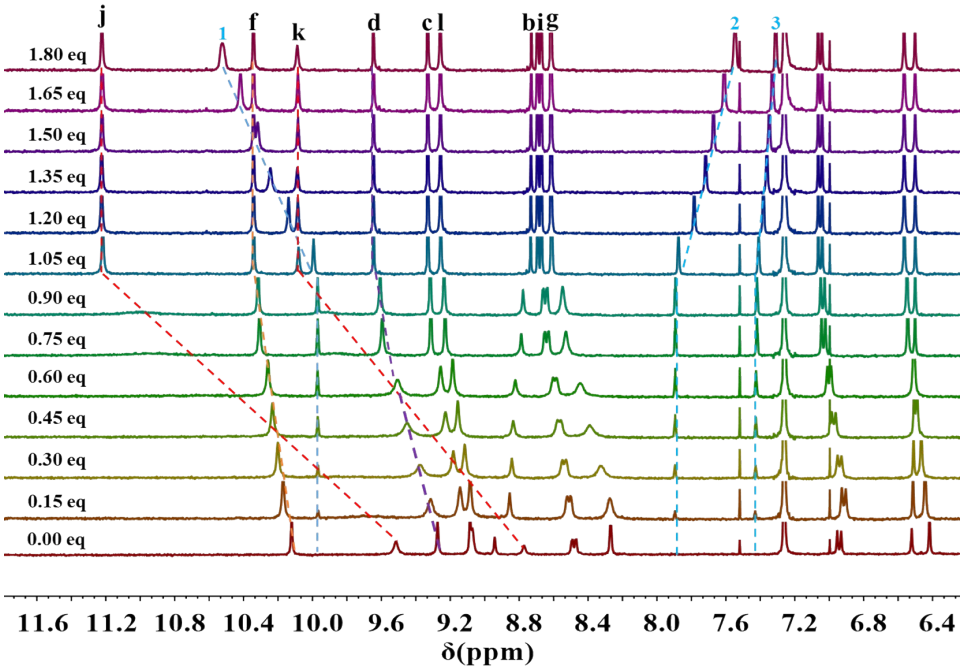

Figure S35. Stacked partial ^{1}H NMR spectra of (a) **1a** (1.0 mM) and (b) with EMIMCl at different concentration in $CDCl_3$ (400 MHz, 298 K).

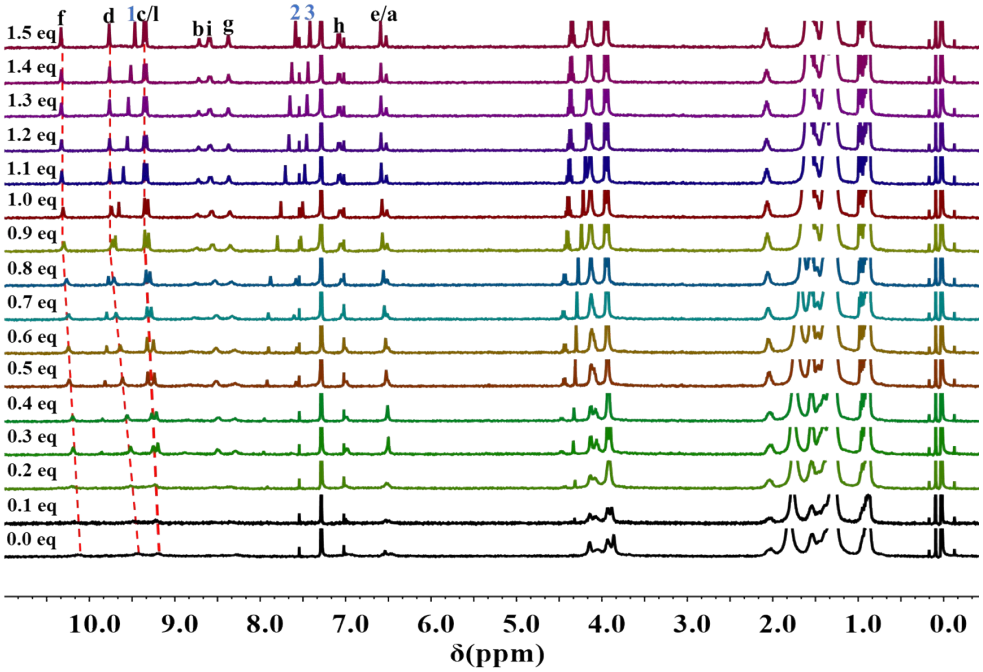

Figure S36. Stacked ^{1}H NMR spectra of (a) **1a** (1.0 mM) and (b) with $EMIMBF_4$ at different concentration in $CDCl_3$ (400 MHz, 298 K).

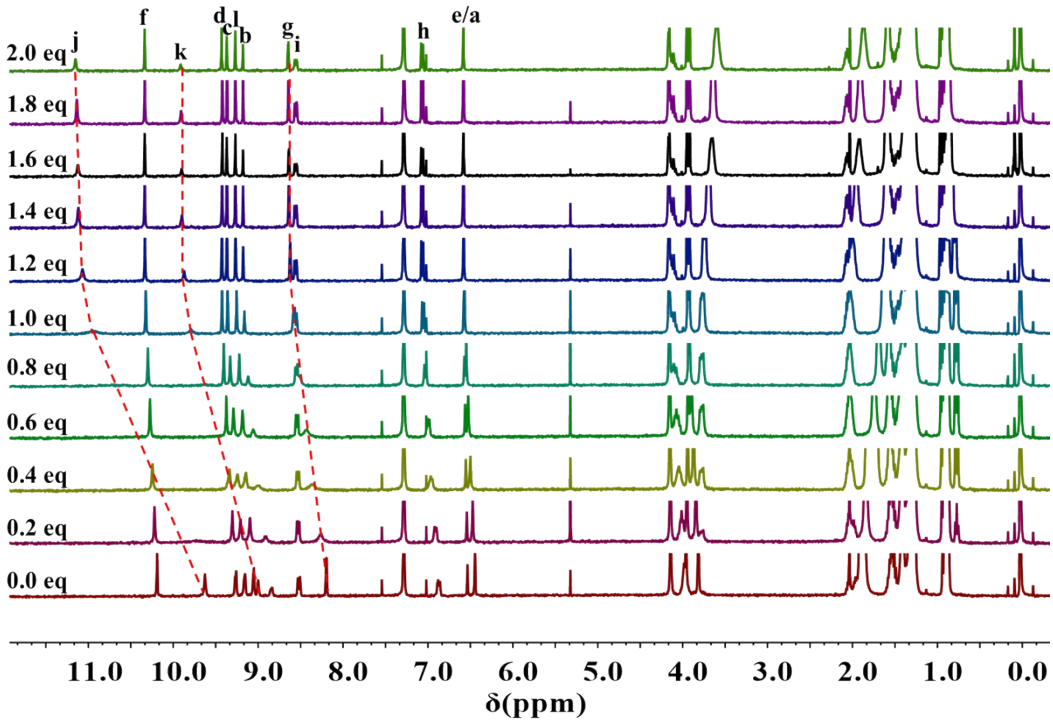

Figure S37. Stacked ^{1}H NMR spectra of (a) **1a** (1.0 mM) and (b) with TBABr at different concentration in $CDCl_3$ (400 MHz, 298 K).

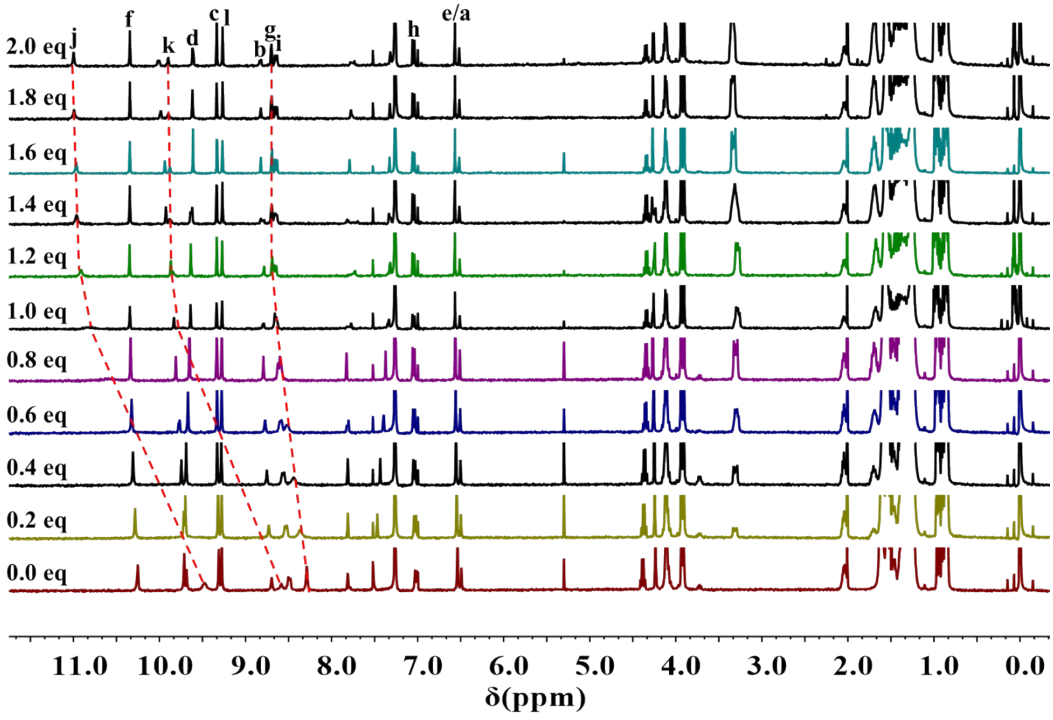

Figure S38. Stacked ^{1}H NMR spectra of (a) **1a** ⊃ $EMIMBF_4$ (1.0 mM) and (b) with TBABr at different concentration in $CDCl_3$ (400 MHz, 298 K).

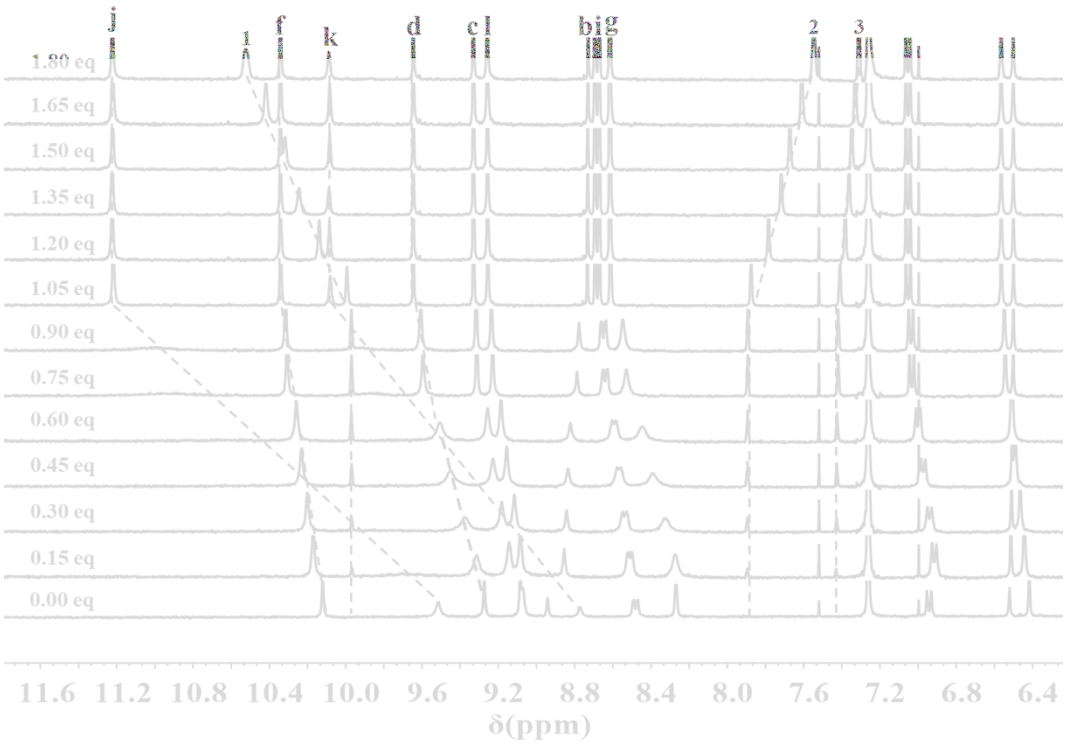

Figure S39. Stacked ^{1}H NMR spectra of (a) **1a** (1.0 mM) and (b) with EMIMCl at different concentration in $CDCl_3$ (400 MHz, 298 K).

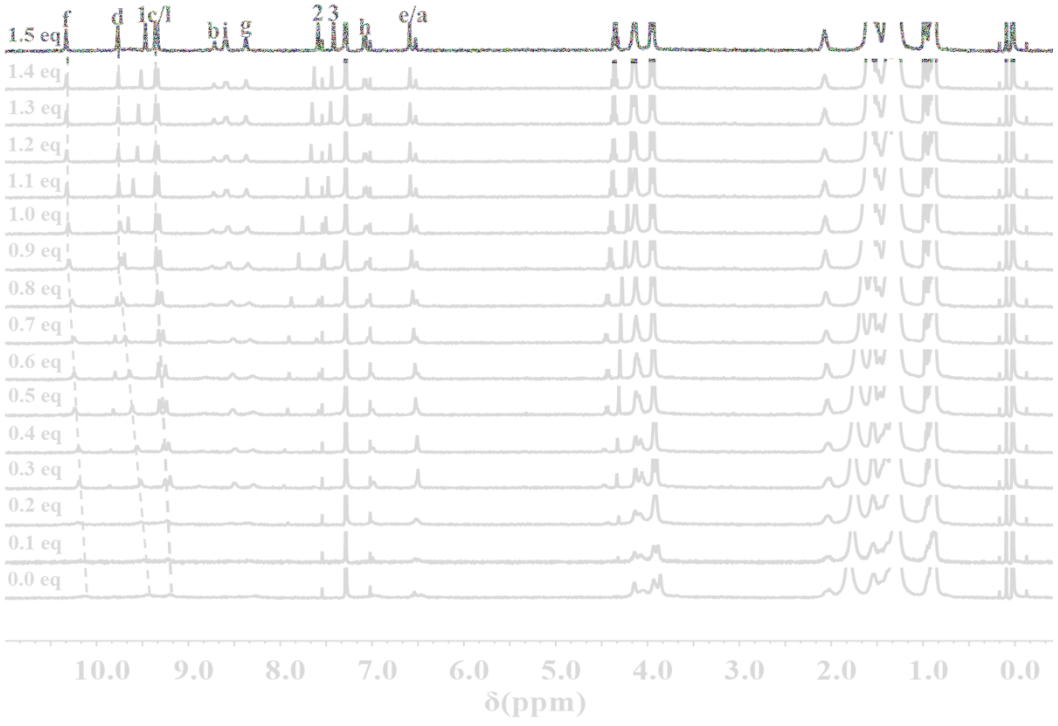

Figure S40. Stacked ^{1}H NMR spectra of (a) **1b** (1.0 mM) and (b) with $EMIMBF_4$ at different concentration in $CDCl_3$ (400 MHz, 298 K).

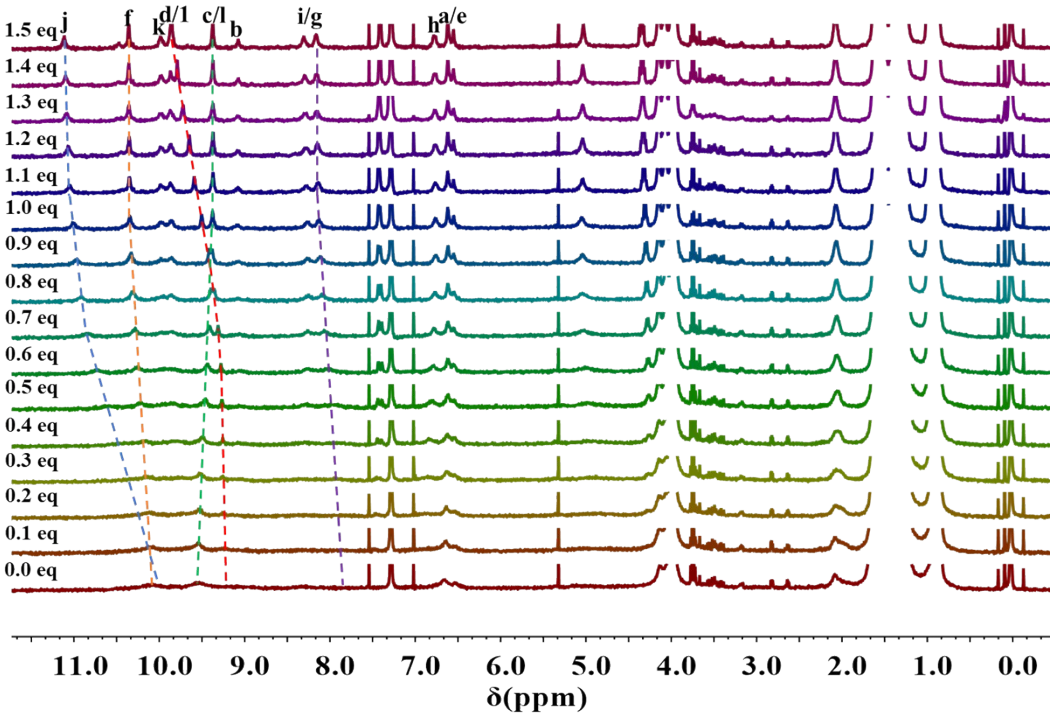

Figure S41. Stacked ^{1}H NMR spectra of (a) **1b** (1.0 mM) and (b) with EMIMCl at different concentration in $CDCl_3$ (400 MHz, 298 K).

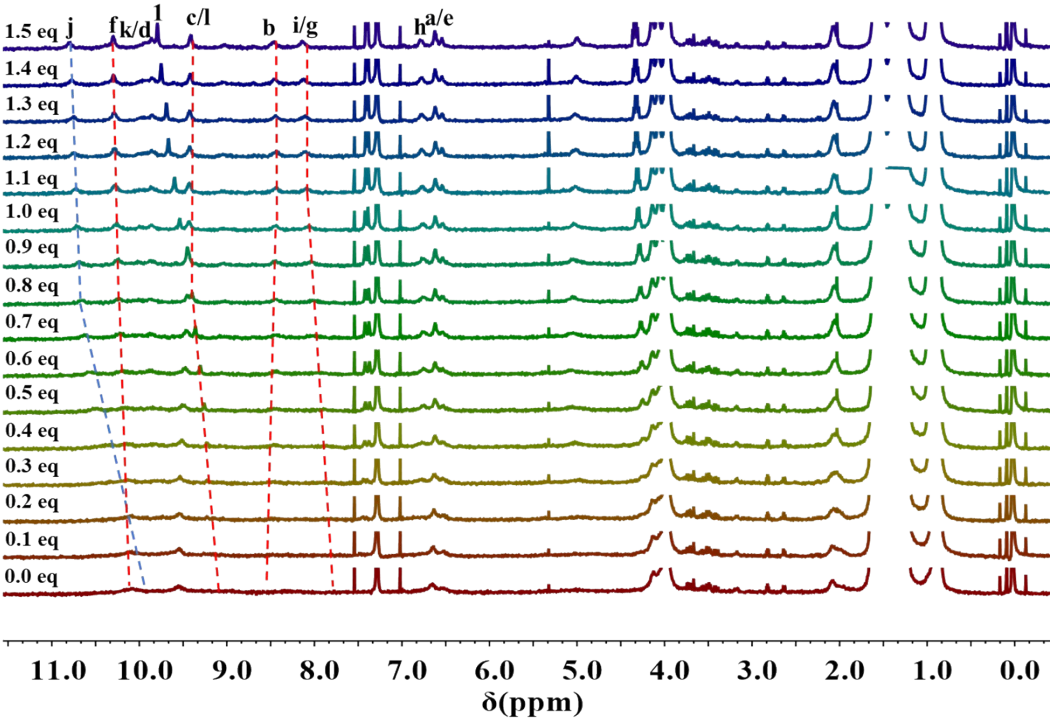

Figure S42. Stacked ^{1}H NMR spectra of (a) **1a** (1.0 mM) and (b) with EMIMBr at different concentration in $CDCl_3$ (400 MHz, 298 K).

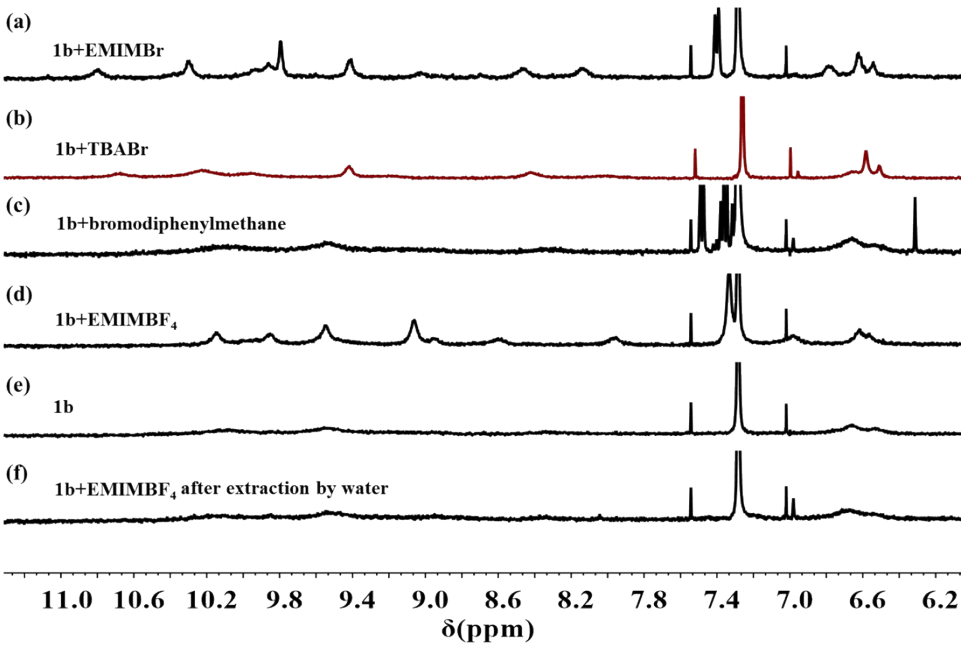

Figure S43. Stacked partial ^{1}H NMR spectra of (a) **1b** + 1.5 equiv of EMIMBr, (b) **1b** + 1.5 equiv of TBABr, (c) **1b** + 1.5 equiv of bromodiphenylmethane, (d) **1b** + 1.5 equiv of $EMIMBF_4$, (e) **1b,** (f) **1b** + 1.5 equiv of $EMIMBF_4$ then washed by H_2O (1.0 mM, $CDCl_3$, 400 MHz, 298K).